International Journal of Thermophysics, Vol. 22, No. 5, September 2001 (© 2001)

The Spectral Directional Emissivity of Photovoltaic Surfaces[1]

D. Labuhn[2] and S. Kabelac[3, 4]

Photovoltaic solar cells are used for the direct conversion of solar radiation to electric power. To evaluate the efficiency of this energy conversion process, all in- and outgoing fluxes in the thermodynamic balance equations for energy and entropy must be known. The spatial and spectral distribution of radiation energy intensities must be known to calculate the radiation energy fluxes. To calculate the entropy fluxes, additional information on the coherence properties of the radiation field is essential. This information is expressed by the degree of polarization. First results of measurements of the optical properties of a solar cell are presented. The calculation procedure to obtain the outgoing energy and entropy fluxes is described. The experimental apparatus introduced in this paper yields the spectral directional emissivity by comparing the sample radiation with the radiation from an isothermal cavity. The degree of polarization of the emitted radiation is determined by a retarder/polarizer set within the apparatus. Both quantities are measured in the infrared region for wavelengths between 4.0 and 20.0 μm.

KEY WORDS: degree of polarization; emissivity; radiation entropy; solar cell.

1. INTRODUCTION

The solar energy flux which reaches the terrestrial surface after passing through the atmosphere in the form of electromagnetic radiation is accompanied by an entropy flux. This entropy results, on the one hand, from the spatial divergence of the propagating electromagnetic wave and,

[1] Paper presented at the Fourteenth Symposium on Thermophysical Properties, June 25–30, 2000, Boulder, Colorado, U.S.A.

[2] OHB-System GmbH, Universitätsallee 27–29, D-28359 Bremen, Germany.

[3] Institut für Thermodynamik, Universität der Bundeswehr Hamburg, D-22039 Hamburg, Germany.

[4] To whom correspondence should be addressed. E-mail: Kabelac@unibw-hamburg.de.

0195-928X/01/0900-1577/0 © 2001 Plenum Publishing Corporation

on the other hand, from its wavelength dispersion. When incoming radiation energy is converted to electrical energy, as is the case in devices which employ the photovoltaic effect, the incoming entropy flux has to be conveyed to the environment, including the entropy produced within the device. This holds if a steady-state condition is assumed. The energetic and exergetic energy conversion efficiencies depend decisively on the success of the entropy removal because an entropy flux always adheres to an energy flux which then is lost for the conversion output. As the electrical energy (as well as the mechanical energy) is free of entropy, the removal of the entropy flux has to be realized by means of a heat loss or by the outgoing radiation flux. Maximum energetic conversion efficiencies $\eta = P_{el}/(Ae_{in})$ for solar radiation, i.e., the outgoing electric power P_{el} divided by the incoming radiation energy flux density e_{in} and the area A of the surface, have been discussed, for example, by deVos and Pauwels [1], Landsberg and Tonge [2], and Kabelac [3]. Their theoretical values lie between $0.5 < \eta < 0.85$ depending on the entropy content of the incoming radiation and the model used. The entropy content of a radiation energy flux depends on its spectral and directional distribution, as was discussed by Kabelac and Drake [6].

Real conversion efficiencies are much lower than the maximum possible values. Very good solar cells reach values around $\eta = 0.25$ under laboratory conditions. To exceed the value $\eta = 0.3$, mechanically stacked tandem concentrator solar cells are being developed. The reasons for this depletion are the intrinsic properties of the material involved and the optical properties, i.e., the emissivity and reflectance of the surface of the conversion device that interacts with the incoming radiation.

The aim of this paper is to describe, by means of thermodynamic balance equations, the influence of the optical properties of a radiation energy conversion device on the energetic conversion efficiency. To be more specific, a solar cell is used as an example device. Once these dependences are understood, criteria for the optimum optical properties for the best conversion efficiencies can be proposed from a thermodynamic point of view.

The way the solar cell is modeled is shown in Fig. 1. Radiation energy flux densities are denoted e, and entropy flux densities d. The arrows indicating the energy fluxes show the respective content of available energy. Electric power is pure availability, while the availability of a heat flux is given by the Carnot factor $\eta_C = 1 - T/T_{amb}$. The electric power P_{el} is calculated from the energy balance equation,

$$0 = A(e_{in} - e_{out}) - \dot{Q} - P_{el} \tag{1}$$

and the entropy balance equation,

$$0 = A(d_{\text{in}} - d_{\text{out}}) - \frac{\dot{Q}}{T} + A\dot{s}_{\text{irr}} \tag{2}$$

for this simple converter, where $\dot{s}_{\text{irr}}$ is the entropy production rate per surface area. A denotes the photovoltaic active area of the cell. After elimination of the heat flux $\dot{Q}$, these equations result in

$$P_{\text{el}}/A = e_{\text{in}} - e_{\text{out}} + T(d_{\text{out}} - d_{\text{in}}) - T\dot{s}_{\text{irr}} \tag{3}$$

where T is the temperature at which the heat flux $\dot{Q}$ leaves the device. It is evident from Eq. (3) that the power output P_{el} will increase if the outgoing entropy flux $A \cdot d_{\text{out}}$ is raised as high as possible without changing the outgoing energy flux $A \cdot e_{\text{out}}$. The product $T \cdot \dot{s}_{\text{irr}}$ will diminish the power output.

For a solar energy converter, the necessary data about the incoming radiation can be obtained from atmospheric models [4]. Additionally, information on the polarization of this radiation, i.e., due to scattering, has to be provided to allow the calculation of the incoming radiation entropy flux. This procedure is summarized in Section 2.

The radiation leaving the converter consists of the reflected part of the incoming radiation and of the radiation emitted by the surface itself. To calculate the energy and the entropy flux leaving the converter, its surface temperature and its optical properties, e.g., the emissivity, reflectance, and bidirectional reflection function (BDRF), must be known.

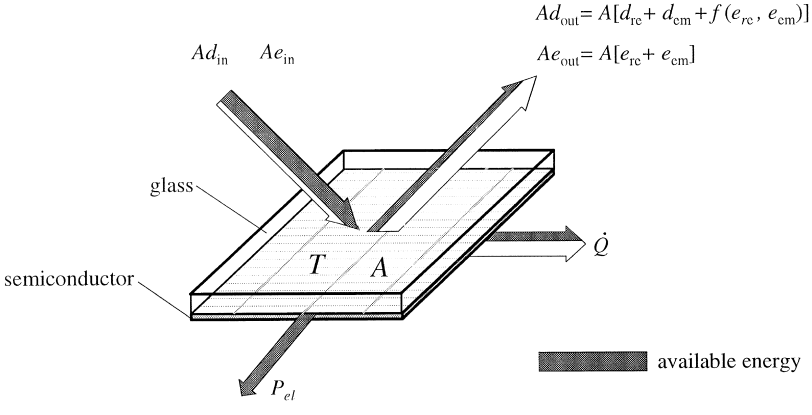

Fig. 1. Simple model of a solar cell, with the energy fluxes depicted by arrows.

From the energetic point of view, the radiation energy exchange in the infrared sometimes seems negligible, but this does not hold true for the entropy, which is also transported with infrared radiation. Therefore, information on the spectral directional optical properties of the interacting surface is necessary for all directions and for all wavelengths of thermal radiation. Reliable data sets are scarce and often compiled by different authors for different regions of wavelength, which results in inconsistent data sets.

In this paper, the basic equations needed to calculate radiation energy and entropy fluxes are reviewed and the dependency of reflected and emitted radiation entropy on the optical properties of a surface is discussed. An apparatus is presented which is capable of measuring the spectral directional emissivity and the degree of polarization in the infrared. In contrast to energy calculations, the degree of polarization is an important input function for entropy calculations because it describes coherence properties of the radiation field.

2. THE RADIATION ENTROPY EQUATION

In this section the basic equations for the calculation of radiation energy and entropy fluxes from the spectral and directional distribution of the radiation energy intensity $L_\lambda = L_\lambda(\lambda, \Omega)$ and the degree of polarization $\Pi = \Pi(\lambda, \Omega)$ of the quasi-monochromatic ray pencils are reviewed for further discussion. In this context "quasi-monochromatic" means that energy is transported in a small wavelength interval, $\mathrm{d}\lambda$, with $\mathrm{d}\lambda/\lambda \ll 1$.

Radiation energy and entropy fluxes per unit area can be calculated from the double integrals

$$e = \int_{\Omega=0}^{\Omega=2\pi} \int_{\lambda=0}^{\lambda=\infty} L_\lambda \cos\vartheta \, \mathrm{d}\lambda \, \mathrm{d}\Omega \qquad \text{and} \qquad d = \int_{\Omega=0}^{\Omega=2\pi} \int_{\lambda=0}^{\lambda=\infty} K_\lambda \cos\vartheta \, \mathrm{d}\lambda \, \mathrm{d}\Omega \tag{4}$$

of the spectral radiation energy intensity L_λ and the spectral radiation entropy intensity K_λ with respect to the wavelength over the entire spectrum $0 \leqslant \lambda < \infty$ and to the solid angle of the entire hemisphere $\Omega = 2\pi$. The zenith angle ϑ is the sharp angle between the direction of the radiation from $\mathrm{d}\Omega$ and the normal vector to the surface element.

To calculate the radiation entropy intensity K_λ, the radiation temperature must be known. The Planck equation used to calculate the spectral

radiation intensity that a blackbody with a uniform surface temperature T emits into vacuum can be solved for temperature:

$$T = \frac{hc}{k\lambda} \frac{1}{\ln\left[2hc^2/(\lambda^5 L_\lambda^{\mathrm{b}}) + 1\right]} \tag{5}$$

In Eq. (5) k is the Boltzmann constant, h is the Planck constant, and c is the speed of light in vacuum. For blackbody radiation the spectral radiation temperature T is independent of the wavelength, which is not the case for arbitrary radiation. Even scaled-down or diluted blackbody radiation, often called gray radiation, results in different spectral radiation temperatures for each wavelength as shown by Landsberg and Tonge [5]. According to Callen [7] each individual spectral ray pencil may be treated as a thermodynamic phase under equilibrium conditions. In this case, the Gibbs fundamental equation,

$$\partial K_\lambda = \frac{1}{T_\lambda} \partial L_\lambda \tag{6}$$

can be written for a spectral ray pencil, provided that photons do not interact with each other. This equation holds for equilibrium radiation as it exists in an isothermal cavity, i.e., blackbody radiation. It has to be extended from the unpolarized equilibrium case to the case where, in general, partially polarized nonequilibrium radiation fluxes (see, i.e., Ref. 6).

Integration of Eq. (6) with respect to wavelength for completely polarized radiation with intensities $L_\lambda^{\min}$ and $L_\lambda^{\max}$, respectively, yields

$$K_\lambda^{\mathrm{pol}} = \frac{kc}{\lambda^4}\left[\left(1 + \frac{\lambda^5 L_\lambda^{\min_{\max}}}{hc^2}\right)\ln\left(1 + \frac{\lambda^5 L_\lambda^{\min_{\max}}}{hc^2}\right) - \left(\frac{\lambda^5 L_\lambda^{\min_{\max}}}{hc^2}\right)\ln\left(\frac{\lambda^5 L_\lambda^{\min_{\max}}}{hc^2}\right)\right] \tag{7}$$

This equation is valid for completely polarized radiation only. The spectral radiation energy intensity L_λ with an arbitrary degree of polarization Π can be split mentally into two completely polarized and mutually independent parts,

$$L_\lambda^{\min} = L_\lambda \frac{1 - \Pi}{2} \qquad \text{and} \qquad L_\lambda^{\max} = L_\lambda \frac{1 + \Pi}{2} \tag{8}$$

In this case, the spectral radiation entropy intensity is

$$K_\lambda = K_\lambda^{\mathrm{pol}}(L_\lambda^{\min}) + K_\lambda^{\mathrm{pol}}(L_\lambda^{\max}) \tag{9}$$

because both intensities are eigenvalues of the ray pencil's coherency matrix and, consequently, mutually independent and thus additive [8]. In all other cases, a coherency term, f (see Fig. 1), must be considered.

The degree of polarization Π introduced here is defined as the polarized part of the spectral radiation intensity divided by its total intensity. $\Pi = 0$ denotes unpolarized and $\Pi = 1$ completely polarized radiation. Further information about the polarization state can be obtained from the Stokes vector $\mathbf{S}$, whose four elements are real quantities and accessible to measurements. From the elements of the Stokes vector, the degree of polarization,

$$\Pi = \frac{\sqrt{S_1^2 + S_2^2 + S_3^2}}{S_0} \tag{10}$$

can easily be calculated. S_0 is the intensity of the beam under consideration, whereas S_1, S_2, and S_3 are used to describe its state of polarization (linear, circular, or elliptical).

In this context, special consideration must be given to the expression "quasi-monochromatic." If the radiation were strictly monochromatic, it would consist of one single wavelength. The two subbeams would have a constant phase difference, and the amplitudes would be time invariant. These subbeams are then said to be completely coherent and thus free of radiation entropy. In the case of quasi-monochromatic radiation the phase difference and the amplitudes vary slowly compared to the time period of the radiation but rapidly in comparison to any observation time. The parameter S_0 is defined as the sum of the amplitudes in the orthogonal beam directions, whereas S_1 is the difference of these quantities. By means of setting one of the subbeam's intensities equal to zero, complete polarization with $S_0 = S_1$ can be achieved, independently of any phase relation. Using Eqs. (7)–(9), the radiation entropy intensity of arbitrary radiation can be calculated.

3. EXPERIMENTAL

To evaluate energy and entropy balances of devices that exchange energy and entropy with their environment by means of electromagnetic radiation, the radiation energy intensities $L_\lambda = L_\lambda(\lambda, \Omega)$ and the respective degree of polarization $\Pi = \Pi(\lambda, \Omega)$ of all incoming and outgoing radiation fluxes must be known. The wavelengths of interest on behalf of a solar cell cover the short-wave part of the spectrum for the incoming and reflected radiation and the long-wave infrared part for the emitted radiation. As

spectral radiation incident upon an opaque surface element from a particular direction is either absorbed or reflected, the respective parts are related by the law of conservation of energy:

$$1 = \varrho'_\lambda + \alpha'_\lambda \qquad \text{or} \qquad 1 = \varrho'_\lambda + \varepsilon'_\lambda \tag{11}$$

The reflected radiation part is represented by the spectral directional reflectance ϱ'_λ and the absorbed radiation can be calculated from the spectral directional absorptance α'_λ, which is related to the spectral directional emissivity by Kirchhoff's law $\alpha'_\lambda = \varepsilon'_\lambda$. To characterize the radiative behavior of a nontransparent surface element from the energetic point of view, knowledge of either the spectral directional emissivity or the reflectance is sufficient. The spectral directional emissivity ε'_λ is defined as the ratio of the spectral radiation intensity L_λ emitted by the surface element to the spectral radiation intensity of a blackbody L^{b}_λ at temperature T. The emitted spectral radiation energy intensity can be calculated from the Planck equation and the spectral directional emissivity ε'_λ, which results in

$$L_\lambda = \varepsilon'_\lambda L^{\mathrm{b}}_\lambda = \frac{2hc^2}{\lambda^5} \frac{\varepsilon'_\lambda}{\exp[hc/(k\lambda T)]-1} \tag{12}$$

In the infrared wavelength range from 4.0 to 20.0 μm, measurements of the spectral directional emissivity have been performed radiometrically by comparing the spectral radiation energy coming from the sample surface with a blackbody source at the same temperature. The temperature range for both objects is from $T_{\min} = 373.15$ K to $T_{\max} = 473.15$ K. Temperature measurements are made with calibrated resistance thermometers and controlled by means of two independent PID controllers. The maximum deviation between the two temperatures observed during the measurements was less than 0.3 K. The radiation is received by a FTIR spectrometer with a highly linear semiconductor detector. A schematic of the apparatus used is shown in Fig. 2. The sample chamber is maintained at $T = 285.15$ K, which is also the optimal operating temperature of the spectrometer. The temperatures are kept at the same level to avoid corrections of blackbody radiation. To measure the emissivity as a function of the zenith angle, the sample and its heating system are swivel mounted. The angle resolution is better than 0.01°, and the reproducibility is better than 0.1°. The accessible zenith angle is limited to 70° by the ratio of the area the spectrometer views on the sample surface and the sample surface area. The sample diameter is 150 mm, and the measurement spot diameter is 20 mm. The overall uncertainty of emissivity measurements is estimated to be smaller than 7%, the main cause being temperature fluctuations of the spectrometer.

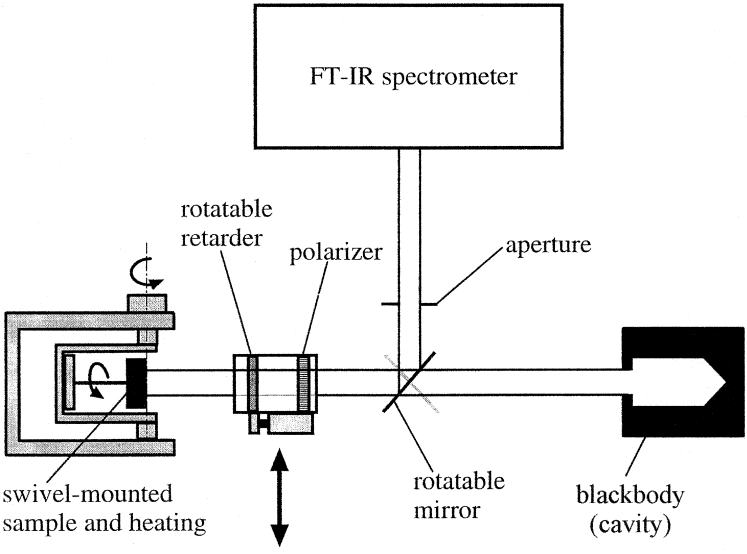

Fig. 2. Apparatus used for measurements of spectral directional emissivity and degree of polarization. To change between the two measurements, the unit containing the retarder and the polarizer can be inserted into or removed from the sample radiation path.

The calculation of radiation entropy fluxes requires the spectral radiation intensity $L_\lambda = L_\lambda(\lambda, \Omega)$ and, in addition, the degree of polarization $\Pi = \Pi(\lambda, \Omega)$, which can be calculated from the Stokes vector in Eq. (10). The measurement of the elements of the Stokes vector is accomplished by means of radiation intensity measurements, which allow the use of the same apparatus as for emissivity measurements with minor modifications of the optical setup. The beam under investigation is propagated through a retarder which produces a phase shift δ. The retarder is rotated continuously; its instantaneous angle is Θ. Subsequently the beam passes through a linear polarizer, as shown in Fig. 3. Fourier analysis of the spectral radiation intensity $\langle E'(t) \rangle$ as a function of the retarder's rotational angle Θ yields the elements of the Stokes vector. This as well as several other methods to measure the degree of polarization are described by Collett [9] and Shurcliff [10]. Uncertainties for these measurements are estimated to be up to 15%. The reason is the time span these measurements take, in comparison to measurements of emissivities. Another reason is the reduction in signal intensity because of the polarizer and the retarder lying in the optical path.

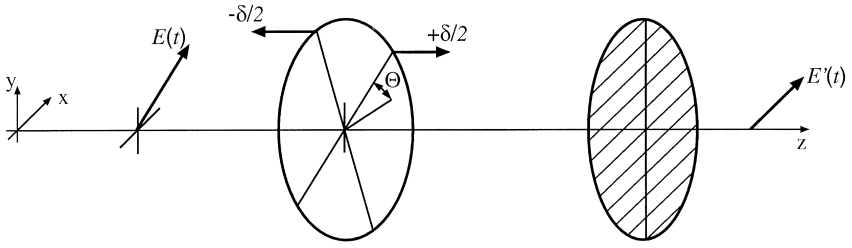

Fig. 3. Measurement principle to obtain the elements of the Stokes vector.

4. DISCUSSION

In this section, the significance of the long-wave part of the spectrum for the entropy balance is analyzed. This is done, as an example, for a common solar cell consisting of the semiconductor material at its backside and a glass layer on the front side. The glass serves as the substrate for the comparatively thin semiconductor layer and as a protective coating against degradation due to mechanical and chemical attacks. The incoming radiation has to pass the glass layer at least once. To approximate terrestrial sunlight, the incident direct solar radiation, which is assumed to be unpolarized, is calculated from the model given by Bird and Riordan [12] for an arbitrarily chosen clear sky condition at noon. It is confined to a small solid angle $\Omega_{\text{in}} = 6.81 \times 10^{-5}$ sr at normal orientation to the cell's surface. The values for the incoming energy flux e_{in} and the adherent entropy flux d_{in} are computed using Eqs. (4) and (7)–(9); they are listed in Table I.

Losses of radiation energy intensity may occur because of three mechanisms. The first is reflection of incoming radiation at the air–glass interface. From the incident radiation energy and entropy, 4.6% is reflected at the air–glass interface (e_{re} and d_{re}).

The second mechanism is absorption in the glass bulk material. The absorption coefficient,

$$\alpha = \frac{L_\lambda^{\text{abs}}}{L_\lambda^{\text{in}}} = 1 - \exp\left(-\frac{4\pi}{\lambda} kh\right) \tag{13}$$

is calculated from the energy which is absorbed in the glass, L_λ^{abs} and the energy which enters the glass, L_λ^{in}. In this equation $h = 3$ mm is the path length of the radiation within the material, λ denotes the wavelength in vacuum, and k is the absorption coefficient, which is calculated in a very similar manner as by Born and Wolf [8] from the attenuation index κ.

Table I. Energy and Entropy Fluxes Calculated with the Data of Gray (Model I) and with the Present Measurements (Model II)

Description	Model I	Model II
Incoming radiation energy flux density e_{in} ($W \cdot m^{-2}$)	611.03	611.03
Incoming radiation entropy flux density d_{in} ($W \cdot m^{-2} \cdot K^{-1}$)	0.16	0.16
Reflected radiation energy flux density e_{re} ($W \cdot m^{-2}$)	28.43	28.43
Reflected radiation entropy flux density d_{re} ($W \cdot m^{-2} \cdot K^{-1}$)	0.019	0.019
Absorbed heat		
Glass, $\dot{q}_{gl}$ ($W \cdot m^{-2}$)	5.74	5.74
Semiconductor, $\dot{q}_{sc}$ ($W \cdot m^{-2}$)	456.95	458.10
Generated power P_{el}/A ($W \cdot m^{-2}$)	119.92	118.76
Emitted radiation energy flux e_{em} ($W \cdot m^{-2}$)	165.92	125.03
Emitted radiation entropy flux d_{em} ($W \cdot m^{-2} \cdot K^{-1}$)	0.813	0.621
Lost convective heat $\dot{q}_l$ ($W \cdot m^{-2}$)	296.77	338.81
Lost convective heat entropy $\dot{q}_l/T$ ($W \cdot m^{-2} \cdot K^{-1}$)	0.964	1.093
Temperature T of the cell (K)	307.99	310.09
Entropy production rate $\dot{s}_{irr}$ ($W \cdot m^{-2} \cdot K^{-1}$)	1.634	1.573
Efficiency η (%)	19.63	19.44

The graph in Fig. 4 indicates the index of refraction n and the attenuation index κ for the glass layer as given by Gray [11]. It can be seen that this material is nearly transparent ($\kappa \ll 1$) for solar radiation with wavelengths from 0.3 to 3.6 μm. The radiation flux $\dot{q}_{gl}$ which is absorbed in the glass is also given in Table I.

The third mechanism is absorption of photons with $E_{ph} = h\nu > E_{bg}$ and subsequent conversion to electrical energy. As the influence of the infrared wavelengths on the entropy balance is discussed, the semiconductor is characterized by means of its bandgap energy E_{bg} only. For the amorphous silicon of the cell under investigation, the bandgap energy is $E_{bg} = 1.3$ eV. The part of the incident radiation which reaches the semiconductor layer after passing the glass is L_λ. The energy of photons with wavelengths longer than λ_{bg} is absorbed at the backside of the semiconductor and then converted to inner energy of the solar cell. The same process happens to the energy of photons which create electron-hole pairs in excess of the bandgap energy. It is transformed to the inner energy of the semiconductor material by means of phonons. Both are represented together by the heat

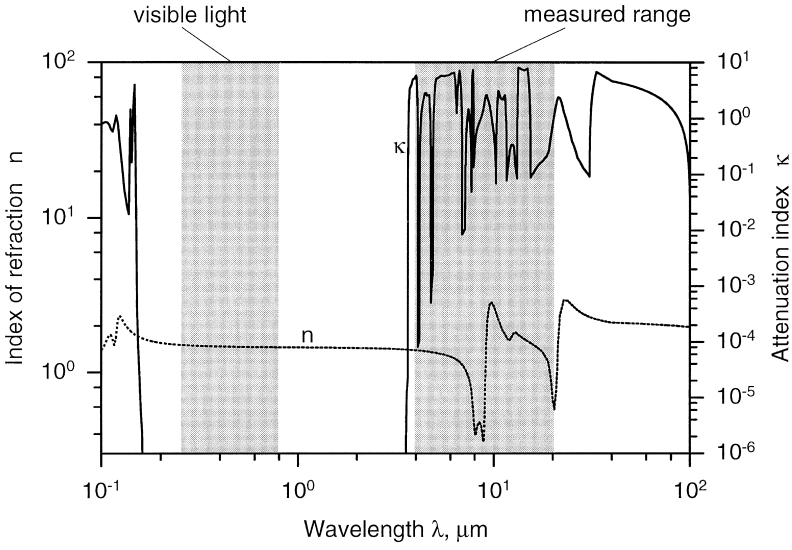

Fig. 4. Values of the index of refraction n and the attenuation index κ for glass given by Gray [11].

flux per surface area $\dot{q}_{sc}$. The remaining photon energy is converted to electrical power,

$$P_{el}/A = (1-p(T)) \int_{\lambda=0}^{\lambda_{bg}} \left(\frac{\lambda}{\lambda_{bg}}\right) L_\lambda \Omega_{in} \, d\lambda . \tag{14}$$

The bandgap wavelength is $\lambda_{bg} = c/\nu_{bg} = ch/E_{bg} = 0.95\ \mu$m. In Eq. (14) the recombination probability of electron-hole pairs is given by the the temperature-dependent coefficient $p(T)$. The recombination is assumed not to be luminescent but to yield internal energy. As the cell performance decreases with temperature, the temperature coefficient for the recombination probability is approximated by $dp/(p\,dT) = -0.2\%\ K^{-1}$.

The energy which is absorbed either in the glass or in the semiconductor is converted to inner energy within the cell. Under a steady-state condition the same amount of energy has to be conveyed to the environment by emission of infrared radiation of the glass layer or by heat convection on both sides of the cell. In this model convective heat losses $\dot{q}_l$ are accounted for by setting the heat transfer coefficient to $h_H = 10\ W \cdot m^{-2} \cdot K^{-1}$, which is suitable for a no-wind condition. To keep the calculations simple, the outside of the cell at the backside surface is treated like a perfect mirror. For all wavelengths the glass is regarded as optically flat because its surface

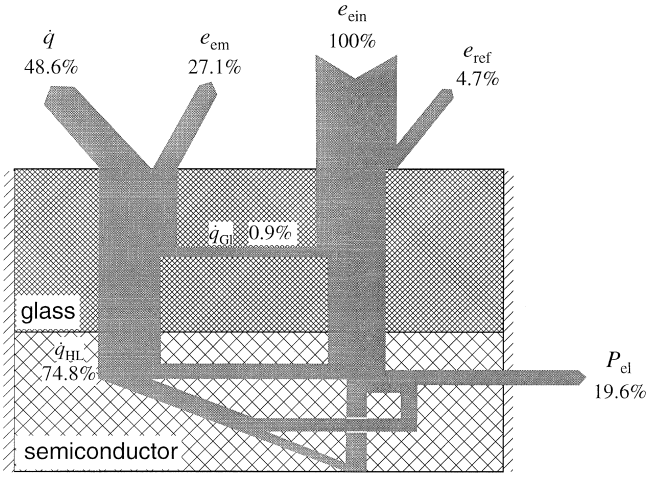

Fig. 5. Energy flow diagram for a simple solar cell (Fig. 1) of Model I under steady-state conditions.

roughness is small compared to the wavelength. Therefore, the emissivity and the degree of polarization of the emitted radiation can be calculated with the Fresnel equations (see Ref. 8) from the index of refraction n and the attenuation index κ in the case where these data are available. Figure 5 summarizes the energy balance for this particular case. Figure 6 shows the corresponding entropy flow diagram.

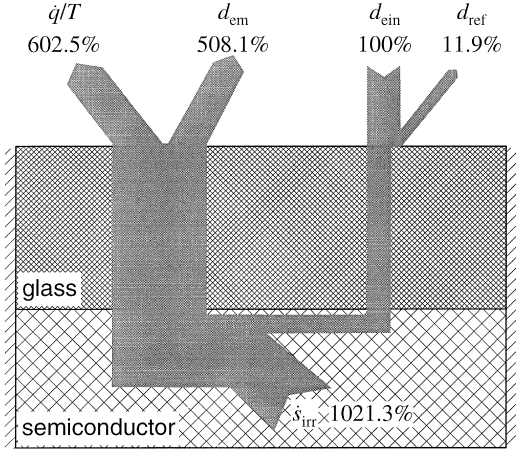

Fig. 6. Entropy flow diagram for a simple solar cell corresponding to Model I.

Two sets of data in the infrared are compared. On the one hand, the data for n and κ given by Gray (see Fig. 4) are referred to as model I. On the other hand, the results for the directional spectral emissivity ε'_λ and the degree of polarization Π from our measurements, which are depicted in Figs. 7a and 7b, respectively, are used (model II). For both calculations the optical properties given by Gray are used in the wavelength range of the visible light.

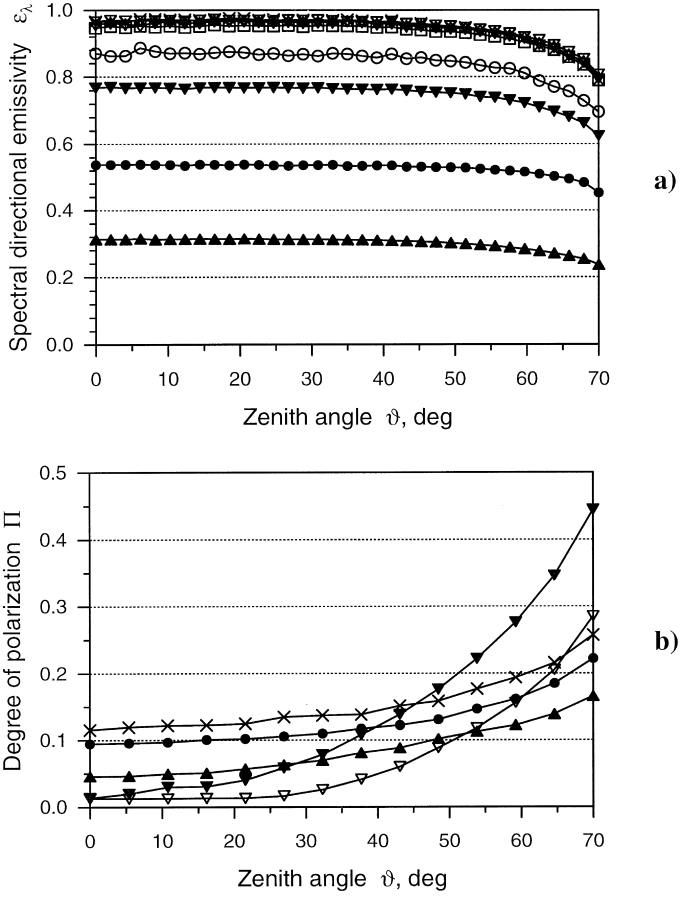

Fig. 7. Emissivities measured radiometrically and the degree of polarization of the emitted radiation for glass used as a protective coating for a solar cell as a function of wavelength. (a) (●) $\lambda = 6.0\ \mu$m; (▲) $\lambda = 8.0\ \mu$m; (▼) $\lambda = 10.0\ \mu$m; (▽) $\lambda = 12.0\ \mu$m; (□) $\lambda = 14.0\ \mu$m; (◇) $\lambda = 16.0\ \mu$m; (×) $\lambda = 18.0\ \mu$m; (○) $\lambda = 20.0\ \mu$m. (b) (×) $\lambda = 4.3\ \mu$m; (●) $\lambda = 5.7\ \mu$m; (▲) $\lambda = 8.0\ \mu$m; (▼) $\lambda = 10.3\ \mu$m; (▽) $\lambda = 12.0\ \mu$m.

For an ambient temperature $T_{amb} = 293.15$ K the balance equation for the energy yields the cell temperature T for both models, the heat lost by convection is $\dot{q}_l$, and the emitted radiation is e_{em}.

It can be seen that the cell temperature depends on the infrared emission properties. As the cell performance decreases with temperature due to $p(T)$, one has to make sure that it is kept as cool as possible, especially under extraterrestrial conditions where no convective losses exist and the effect of energy removal by means of infrared radiation is predominant. The entropy produced within the cell in the case of model I exceeds the value for model II, whereas, for the efficiencies, the ratio is inversed. The entropy production caused by heat losses and by emission of radiation has to be investigated in more detail such that the loss mechanism can be addressed in a more specific manner.

5. CONCLUSIONS

A photovoltaic cell has been analyzed from a thermodynamic viewpoint. Special attention has been given to the entropy balance equation and the entropy fluxes of the incoming and outgoing radiation. As the power output of the cell increases when the entropy of the outgoing radiation is high and the entropy production rate is low, the influence of the optical properties of the photovoltaic surface on the cell efficiency has been discussed.

The spectral directional emissivity and the spectral directional degree of polarization of a glass-coated silicium cell, which are needed to calculate the radiation energy and entropy fluxes, have been measured for zenith angles up to 70° and for wavelengths between 4.0 and 20.0 μm. Other optical properties have been taken from the literature. The fluxes and the conversion efficiency have been calculated for different optical data sets. Even though the analysis given here is at its beginning only, it becomes clear that the efficiency of solar radiation conversion devices can be optimized by adjusting the optical properties of the device to the spectrum of the incoming radiation. Special attention has to be given to the infrared wavelength range. Due to new concepts in surface microstructuring, the emissivity of a surface can be diliberately influenced [13]. If the structure on the surface is periodic, for example, resonances occur at certain wavelengths, resulting in an increased emission at these wavelengths. Further investigation will focus on the entropy production due to the interaction between radiation and the surface material.

ACKNOWLEDGMENT

This work was supported by the Deutsche Forschungsgemeinschaft (DFG) Grant Ka 1211/4.

NOMENCLATURE

Symbol	Unit	Quantity
A	m^2	Surface area
c	$m \cdot s^{-1}$	Speed of light in a vacuum
d	$W \cdot m^{-2} \cdot K^{-1}$	Radiation entropy flux density
e	$W \cdot m^{-2}$	Radiation energy flux density
f	—	Coherence term
h	$J \cdot s^{-1}$	Planck constant
h_H	$W \cdot m^{-2} \cdot K^{-1}$	Convective heat transfer coefficient
k	$J \cdot K^{-1}$	Boltzmann constant
K	$W \cdot m^{-2} \cdot K^{-1} \cdot sr^{-1}$	Radiation entropy intensity
K_λ	$W \cdot m^{-2} \cdot K^{-1} \cdot sr^{-1} \cdot \mu m^{-1}$	Spectral radiation entropy intensity
L	$W \cdot m^{-2} \cdot K^{-1} \cdot sr^{-1}$	Radiation energy intensity
L_λ	$W \cdot m^{-2} \cdot K^{-1} \cdot sr^{-1} \cdot \mu m^{-1}$	Spectral radiation energy intensity
n	—	Index of refraction
P	W	Power
$\dot{Q}$	W	Heat flux
$\dot{q}$	$W \cdot m^{-2}$	Heat flux density
$\dot{s}_{irr}$	$W \cdot m^{-2} \cdot K^{-1}$	Entropy production rate density
S_i	—	Elements of the Stokes vector
T	K	Temperature
α_λ	—	Spectral absorptance
α'_λ	—	Spectral directional absorptance
ε_λ	—	Spectral emissivity
ε'_λ	—	Spectral directional emissivity
λ	μm	Wavelength
η	—	Efficiency
ν	$1 \cdot s^{-1}$	Frequency
ρ_λ	—	Spectral reflectance
ρ'_λ	—	Spectral directional reflectance
σ	$W \cdot m^{-2} \cdot K^{-4}$	Stefan–Boltzmann constant
Θ	rad	Angle of retarder
ϑ	rad	Zenith angle
κ	—	Attenuation index
Π	—	Degree of polarization
Ω	sr	Solid angle

REFERENCES

1. A. deVos and H. Pauwels, *Appl. Phys.* **25**:119 (1981).
2. P. T. Landsberg and G. Tonge, *J. Appl. Phys.* **51**:R1 (1980).

3. S. Kabelac, *Thermodynamik der Strahlung* (Vieweg, Braunschweig, 1994).
4. M. A. Rosen, F. C. Hooper, and A. P. Brunger, *Solar Energy* **43**:281 (1989).
5. P. T. Landsberg and G. Tonge, *J. Phys. A Math. Gen.* **12**:551 (1979).
6. S. Kabelac and F. D. Drake, *Solar Energy* **48**:239 (1992).
7. H. B. Callen, *Thermodynamics and an Introduction to Thermostatistics* (John Wiley, New York, 1985).
8. M. Born and E. Wolf, *Principles of Optics* (Pergamon Press, Oxford, 1987).
9. E. Collett, *Polarized Light, Fundamentals and Applications* (Marcel Dekker, New York, 1992).
10. W. A. Shurcliff, *Polarized Light: Production and Use* (Harvard University Press, Cambridge, MA, 1962).
11. D. E. Gray, *American Institute of Physics Handbook* (McGraw–Hill, New York, 1972).
12. R. Bird and C. Riordan, *J. Climate Appl. Meteorol.* **25**:87 (1986).
13. A. Heinzel, V. Boerner, A. Gombert, V. Wittwer, and J. Luther, *Proc. 4th NREL Thermophotovolt. Generat. of Electr. Conf.,* Denver, CO (1998).